Resonance lineshapes in quasi-one-dimensional scattering

Jens U. Nöckel* and A. Douglas Stone

Applied Physics, Yale University

P.O. Box 208284, Yale Station, New Haven CT 06520-8284

*_Current address_:

Department of Physics, University of Oregon, 1371 E 13th Avenue, Eugene, OR 97403

In various recent model calculations on the transport properties of microstructures, transmission resonances have been found that exhibit the asymmetric Fano lineshape. In particular one often encounters points of vanishing transmission or reflection as a resonance is crossed. The interference effects that cause this phenomenon are identified in this paper using first a coupled-channel theory that starts from the full scattering Hamiltonian, and secondly a more general S-matrix approach. The latter is model-independent and thus yields predictions for the possible lineshapes in a wide variety of systems. Model-independent results are desirable because knowledge of the microstructure potentials is often incomplete. We show for the most general multiprobe, multisubband structure that the total transmssion never varies by more than unity on resonance, generalizing a result previously known only for resonant tunneling structures. The role of symmetry is investigated to clarify which features (e.g. reflection zeros) are a consequence of special invariance properties and which are robust in the unsymmetric case. The effect of a resonance is found to decrease with increasing number of leads in a rotationally symmetric structure. Only in a two-probe geometry can zeros in transmission and reflection occur together for a single resonance. The known result that resonances in symmetric resonant tunneling devices always display exactly unit variation of the transmission is shown to be violated in structures where the nonresonant transmission exceeds one. Time reversal invariance is not required in the present treatment. Two model systems displaying asymmetric resonances are discussed. Their advantage is that the resonance lifetime can be tuned externally, making it possible to test a scaling property of the Fano lineshape that we derive below.
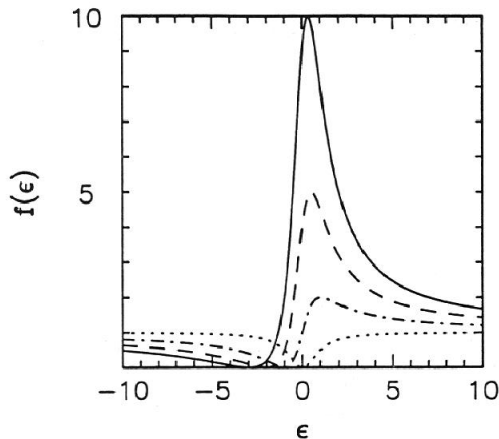
Contents

Figure 1: The Fano lineshape, Eq. (1), for various values of the parameter q.

1. INTRODUCTION

A relatively new arena has been opened for the quantum theory of scattering since it became clear that the electrical linear response of open multiterminal conductors can be related to its transmission and reflection properties.[1] While three-dimensional (3D) scattering theory is well-developed, the confining potentials defining a microstructure force us to consider the scattering of particles whose asymptotic motion is not free. In the absence of magnetic fields, these systems can be called "electron waveguides". A scattering theory for such systems of reduced dimensionality must take into account the different boundary conditions for the stationary states, as well as the different symmetries that play a role. In spherically symmetric 3D scattering, angular momentum is a good quantum number and serves to reduce the problem to a one-dimensional equation for the radial wavefunction. The presence of leads in a microstructure makes it impossible to retain a continuous rotation symmetry. Even if some other set of conserved quantities exists such that the time-independent Schrödinger equation of the system is completely separable, the resulting purely one-dimensional scattering problem obeys different boundary conditions than the radial problem in 3D. In general, separability cannot be expected, and only the asymptotic motion in the leads is of a one-dimensional nature if we consider the leads as semi-infinite and straight. We use the term quasi-one dimensional (Q1D) to emphasize this fact. A motivation for pursuing the formulation of a Q1D scattering theory can be drawn from numerical studies of such systems [2, 3, 4, 5, 6, 7, 8, 9, 10, 11]. Elastic scattering resonances in Q1D systems do not always exhibit the symmetric Breit-Wigner (BW) lineshape familiar from 3D scattering, but instead show an asymmetric lineshape when the nonresonant transmission is significant. Often, but *not* always [2, 7] (cf. Section 2.3), these resonances can be explained in terms of coupling between a bound state and a continuum in different subbands of the quantum wire leads.

Although the Breit-Wigner peak [12] is the most common resonance lineshape ob-

3

served in atomic and nuclear scattering, it has been known for some time that the most general resonant lineshape (which includes the BW as a special case) is described by the asymmetric Fano function, see Fig. (1):

$$f(\epsilon) = \frac{(\epsilon + q)^2}{\epsilon^2 + 1}. \tag{1}$$

Here, $\epsilon = (E - E_R)/\Gamma$ is the (dimensionless) energy from resonance, Γ is the resonance width, and q is the asymmetry parameter. Strongly asymmetric Fano lineshapes are familiar for inelastic autoionizing resonances in atoms[13]; however Simpson and Fano[14] explicitly noted their occurence in spherically-symmetric *elastic* scattering in 1963. In fact this lineshape is implicit in much earlier work in nuclear scattering where strong asymmetries were measured in elastic neutron scattering [15, 16]. To be precise one finds [14] that the elastic scattering partial cross-section near a resonance in angular momentum channel l (neglecting spin) has the form

$$\sigma_l = \frac{2\pi\hbar^2}{p^2} (2l+1) \sin^2 \bar{\theta}_l \frac{(\epsilon - \cot \bar{\theta}_l)^2}{\epsilon^2 + 1}, \tag{2}$$

with p denoting the particle momentum and $\bar{\theta}_l$ the background phase shift in the absence of the resonance. Hence σ_l is proportional to the Fano function with $q = -\cot \bar{\theta}_l$. The only assumption needed is that $\bar{\theta}_l$ is roughly constant with energy across the resonance. Here we see explicitly that in the limit $\bar{\theta}_l \to 0$ ($q \to \infty$) of small background phase shift one recovers the Breit-Wigner lineshape; whereas $q \to 0$ yields a symmetric anti-resonance (BW dip, known in photoabsorption as a window resonance [17]). Note that in the spherically symmetric case σ_l varies between zero and $2\pi\hbar^2 (2l+1)/p^2$, the minimum and maximum values allowed by unitarity of the S-matrix. In particular, the cross section vanishes at $\epsilon = -q$.

In the inelastic case, the characteristic asymmetry with an absorption zero has the well-known interpretation of interference between transition amplitudes from a bound initial state to an unbound final state either directly or via a quasibound (autoionizing) intermediate state. A similar interpretation applies for asymmetric elastic resonances in which scattering via a quasi-bound level interferes with direct (potential) scattering. An important feature of elastic Fano resonances is that the asymmetry parameter depends only on the background phase-shift and not on the strength of the coupling to the quasi-bound level; i. e. , if one could tune this coupling without changing the background scattering the resulting lineshapes should all scale onto the same curve given by Eq. (1). Such an experiment has not been done yet, but may be possible for the first time in a solid-state device [18].

We can categorize the previous work on Q1D resonace phenomena according to the two main goals that are being pursued. Firstly, it is of interest to establish a connection between the lineshape and physical parameters determining the actual mechanism that gives rise to the resonance (such as matrix elements of the scattering potential). Secondly, one may seek general statements about possible lineshape features (e.g. regarding the limits within which the transmission can vary) which are independent of

details of the underlying model. The latter is of particular value in microstructures where a complete knowledge of the potentials is often unattainable. Both goals could be reached simultaneously if all Q1D resonances were describable by a single generic model system in which only a few parameters are unknown. Solving that model would then be tantamount to solving the general problem.

In a recent paper [11], Tekman and Bagwell used a two-band model with a delta function coupling potential to reproduce asymmetric resonances of the type seen in numerical simulations. The lineshape derived in that model calculation is indeed well approximated by Eq. (1). A more general two-band approach for arbitrary coupling potentials has been used by Gurvitz and Levinson [19], but only symmetric lineshapes were considered. These models do not describe resonance phenomena in structures with more than one propagating subband per lead, or with more than two leads. We explore in Section 2 the maximum range of validity of the two-channel model used by Gurvitz and Levinson, which we recognize as a reformulation of Feshbach's theory of coupled scattering channels [20]. The microscopic expressions that we obtain for the Fano lineshape parameters in a generalization of that approach indeed lead us to some predictions that do not depend on the actual potential. But we also show that there are real two-band systems which display Fano resonances and still defy a satisfactory description in terms of the coupled-channel approach of Section 2.

This suggests that general predictions for Q1D resonance lineshapes require a model-independent formalism. A powerful tool in this situation is the S-matrix method, which is also used to derive Eq. (2). In work by Büttiker [21] and other authors [22, 23, 24], various special cases of Q1D scattering are treated by exploiting the analytical properties of the S-matrix. All except the study by Shao *et al.* [24] consider exclusively symmetric (Breit-Wigner) lineshapes. The latter reference, in turn, restricts itself to a single-mode two-probe structure. More than two leads were treated only in Ref. [22] (but only resonant tunneling was considered there).

In Section 3 we provide a general Q1D S-matrix theory for multiprobe, multisubband structures. We first observe that the usual textbook approach leads to wrong predictions, so we have to scrutinize the way in which the connection between quasi-bound states and resonance denominators in the S-matrix is made if there are no continuous symmetries. In the presence of discrete symmetries we derive rigorously the resonance lineshapes for a *multilead* structure in the single-subband regime. Then we investigate the effects of symmetry breaking in two-probe structures with arbitrarily many subbands, and lastly, treat the multilead, multisubband case. Finally, Fano resonances in microstructures have not yet been clearly seen experimentally (although some data taken on quantum point contacts is suggestive [25]); we propose in Section 4 two experiments for observing such resonances and compare numerical model calculations on these systems with the results derived in the preceding Sections.

2. FESHBACH APPROACH

The most obvious difference between Q1D and three-dimensional scattering is the sub-band structure that exists in a quantum wire. At a given energy, particles in the asymptotic region of the wire leads can have different momenta, depending on their subband index. In particular, a bound state in one subband (imaginary wavenumber in the leads) can coexist with an unbound state in another subband. In three-dimensional scattering from a potential that vanishes outside of some scattering region, all incoming and scattered particles have a momentum of the same magnitude if their energy is the same – unless incoming and outgoing particles are of a different kind. The latter case is referred to as multichannel scattering. Although we are dealing with elastic scattering, it is possible to consider the quantum wire as a multichannel system if we treat the different subbands as "channels". The resonances considered in this section are analogous to those arising in multichannel scattering when a closed and an open channel are coupled, the channels in our case being the propagating and cut-off subbands. For completeness and to point out the modifications we have made to the theory, subsection 2.1 contains some material already covered in Ref. [19]. Feshbach's approach has in fact been employed earlier to describe resonances in a waveguide geometry [26], but nonresonant transmission was assumed to be absent.

The Fano function will be derived in this microscopic approach, and an even stronger prediction for the lineshape is given in Subsection 2.2 by making use of inversion symmetry.

2.1. COUPLED-CHANNEL EQUATIONS

We consider a non-uniform quantum wire described by the Schrödinger equation

$$\left[-\frac{\hbar^2}{2m}\nabla^2 + U(x) + W(y) + \hat{V}^{xy} \right] \Psi(x,y) = E\,\Psi(x,y). \tag{3}$$

In the absence of the coupling operator $\hat{V}^{xy}$, the problem is separable and the transverse potential $W(y)$ gives rise to modes $\phi_n(y)$:

$$\left[-\frac{\hbar^2}{2m}\frac{d^2}{dy^2} + W(y) \right] \phi(y) = E_n\,\phi_n(y). \tag{4}$$

Unlike Ref. [19], we do *not* assume $\hat{V}^{xy}$ to be a real local scalar function. This will enable us to investigate if the present approach is applicable to the case of magnetic-field induced coupling [9]. Expanding

$$\Psi(x,y) = \sum_{n=1}^{\infty} \psi_n(x)\phi_n(y), \tag{5}$$

we obtain the coupled-channel equations for $\psi_n(x)$,

$$\left[E - E_n - \hat{K} - U(x) \right] \psi_n(x) = \sum_{l=1}^{\infty} \hat{V}_{nl}\,\psi_l(x), \tag{6}$$

where $\hat{K} \equiv -(\hbar^2/2m)d^2/dx^2$, and the coupling matrix element $\hat{V}_{nl} \equiv \int dy\, \phi_l(y)\, \hat{V}^{xy} \phi_n(y)$ still acts on x. Now choose an energy in the single-subband regime, $E_1 \leq E < E_2$. Provided that the diagonal elements $\hat{V}_{nn}$ vanish far away from the scattering region, only channel $n = 1$ will then have unbound solutions in the absence of off-diagonal coupling:

$$\left[\hat{K} + U(x) + \hat{V}_{11} + E_1 \right] \chi_k^p(x) = E\, \chi_k^p(x), \tag{7}$$

where the index $p = 1, 2$ distinguishes scattering states according to the direction from which the incident wave comes. Specifically, χ_k^p has the asymptotic form

$$\chi_k^p(x) = \begin{cases} t^{bg}\, e^{\pm ikx} & (x \to \pm\infty) \\ e^{\pm ikx} + r_\pm^{bg} e^{\mp ikx} & (x \to \mp\infty) \end{cases} \tag{8}$$

with the upper signs for $p = 1$ (incident wave from the left). The superscript in the transmission and reflection amplitudes t^{bg}, $r_\pm^{bg}$ emphasizes the fact that these scattering states describe the *background* (i.e. nonresonant) scattering in the open channel [27]. Let E be close to the energy of a bound state [28] of the uncoupled channel $n = 2$,

$$\left[\hat{K} + U(x) + \hat{V}_{22} + E_2 \right] \Phi_0(x) = E_0\, \Phi_0(x). \tag{9}$$

If no other channels exhibit bound states in the neighborhood of E_0, we can make the approximation of truncating the sum in Eq. (6) at $n = 2$. The resulting system of equations

$$\left[E - E_1 - \hat{K} - U(x) - \hat{V}_{11} \right] \psi_1(x) = \hat{V}_{12}\, \psi_2(x), \tag{10}$$

$$\left[E - E_2 - \hat{K} - U(x) - \hat{V}_{22} \right] \psi_2(x) = \hat{V}_{21}\, \psi_1(x) \tag{11}$$

is solved in Appendix A using the ansatz [17]

$$\psi_2(x) = A\, \Phi_0(x). \tag{12}$$

This is slightly more direct than the procedure in Ref. [19] because it leads to an exact solution of Eqs. (10), (11) without approximating the Green's function for the second channel and subsequently summing a Born series. The result obtained by the latter method is the same. This ansatz has the physical interpretation that the probability amplitude of the metastable state is dominated by the original bound state wavefunction. From the asymptotic form of the resulting ψ_1 for $x \to \infty$, we can extract the transmission,

$$T = |t^{bg}|^2\, \frac{(E - E_R + \delta)^2}{(E - E_R)^2 + \Gamma^2}. \tag{13}$$

Instead of the original bound-state energy E_0, a shifted *quasibound*-state energy $E_R \equiv E_0 + \Delta$ appears in this expression, due to the real part Δ of the self energy acquired by the bound state. The real quantity δ determines the asymmetry of the lineshape. Defining reduced variables

$$\epsilon \equiv \frac{E - E_R}{\Gamma}, \qquad q \equiv \frac{\delta}{\Gamma}, \tag{14}$$

we arrive at the Fano function,

$$T = |t^{bg}|^2 \frac{(\epsilon + q)^2}{\epsilon^2 + 1}. \tag{15}$$

If the asymmetry parameter q vanishes, we obtain a Breit-Wigner dip. Only this case received further attention in Ref. [19], although the Fano lineshape is implicit in that work. A symmetric *peak* in T arises if we take the limit $|q| \to \infty$ with $q^2|t^{bg}|^2 = c^2$ where $c^2 \leq 1$ (as required by $T \leq 1$),

$$T \to c^2 \frac{1}{\epsilon^2 + 1}. \tag{16}$$

This implies that the symmetric peak can occur only if $t^{bg} \to 0$, and that the Breit-Wigner lineshape constitutes a special case of the Fano function that results when the transmission zero occurs infinitely far from resonance. The constant c^2 in Eq. (16) is only constrained to be less than unity. However, in the next Section we show that $c^2 = 1$ if the system has inversion symmetry because then q and t^{bg} are related to each other with no additional free parameters. The preceding discussion already shows that the Fano function with an exact transmission zero is the general lineshape for resonances in the two-channel Feshbach approach.

2.2. INVERSION SYMMETRY

In this subsection, we extend the approach of Ref. [19] in a different direction, in order to make contact with the predictions of the S-matrix theory to be developed later. Not all the parameters $|t^{bg}|^2$, δ, Γ and E_R in Eq. (103) are independent if the problem has inversion symmetry. We shall see in particular that in this case T not only goes through zero but also through unity at resonance. Further, q will be shown to be independent of the coupling matrix elements.

To this end, it is convenient to consider the reflection R and then use current conservation, $R + T = 1$, to deduce relations between the parameters. Inversion symmetry in the Hamiltonian of Eq. (3) implies that the potentials $U(x)$ and $W(y)$ must be symmetric, so that the transverse modes have a definite parity. Since $\hat{V}^{xy}$ has to be invariant under inversion, it follows immediately that the diagonal coupling matrix elements $\hat{V}_{nn}$ are symmetric under $x \to -x$. But this implies that the bound state $\Phi_0(x)$ in Eq. (9) has a definite parity, and that the scattering states in Eq. (7) satisfy $r_+^{bg} = r_-^{bg} \equiv r^{bg}$. The unitarity of the S-matrix for the uncoupled channel $n = 1$ then makes $(t^{bg})^* r^{bg}$ purely imaginary. These observations are used in Appendix B to deduce that δ and Γ are now related by

$$q^2 = \frac{\delta^2}{\Gamma^2} = \left| \frac{r^{bg}}{t^{bg}} \right|^2. \tag{17}$$

The asymmetry parameter q therefore depends only on the background transmission t and not on the two parameters characterizing BW resonances, E_R and Γ. These three are the only parameters needed to determine the lineshape in a symmetric structure,

instead of the four required in the general case of Equation (13), which now takes the form

$$T = \frac{1}{1+q^2} \frac{(E - E_R + q\Gamma)^2}{(E - E_R)^2 + \Gamma^2}. \tag{18}$$

This explicit relation also confirms that Eq. (15) yields a Breit-Wigner dip when the non-resonant transmission is unity, while the other extreme of $t^{bg} \to 0$ leads to a peak of the form

$$T \to \frac{1}{\epsilon^2 + 1}, \tag{19}$$

cf. Eq. (16) with $c^2 = 1$.

2.3. FAILURES OF THE COUPLED-CHANNEL MODEL

One assumption on which the preceding analysis hinges is that the two-channel approximation is valid. But this will break down if the bound state can couple to the scattering state indirectly by way of a transition to one or more intermediate closed channels. In Appendix C of Ref. [19] this case is discussed, and it is found that for one additional channel (e.g. $n = 3$) the coupling matrix element $\hat{V}_{12}$ simply has to be replaced by

$$\hat{V}_{12} + \hat{V}_{13}\,G_3\,\hat{V}_{32} \tag{20}$$

in Eq. (10), likewise for $\hat{V}_{21}$. For additional intermediate channels, terms of higher order in $\hat{V}^{xy}$ appear. Thus the formalism can accomodate this complication.

However, we discovered that the crucial ansatz of Eq. (12) which was successfully employed in Refs. [20, 26, 17] and is equivalent to the treatment in Ref. [19], *breaks down* for certain types of coupling operators. The example we consider is scattering in a quantum wire with a transverse magnetic field, which was studied in Ref. [9]. First let us discuss to what extent we have succeeded in keeping the preceding treatment sufficiently general to be applicable to this model system. Assuming a harmonic quantum wire potential $W(y)$ with force constant $m\omega_0^2$, and choosing the Landau gauge $\mathbf{A} = -By\,\hat{\mathbf{x}}$ to represent a magnetic field $\mathbf{B}$ along the z axis, the Schrödinger equation becomes

$$\left[\frac{1}{2m}\left\{(p_x - m\omega_c y)^2 + p_y^2\right\} + \frac{1}{2}m\omega_0^2 y^2 + U(x)\right]\psi(x,y) = E\,\psi(x,y). \tag{21}$$

Here, $\omega_c = \frac{eB}{mc}$ is the cyclotron frequency, and $U(x)$ is an additional longitudinal potential describing a finite-depth square well of length L,

$$U(x) = -U_0\,\Theta(\frac{L}{2} - |x|). \tag{22}$$

Since $U(x)$ is symmetric, the Hamiltonian in Eq. (21) has inversion symmetry. The coupling operator of Section 2 is now the perturbation due to the magnetic field in Eq. (21),

$$\hat{V}^{xy} = -\omega_c\,y\,p_x + \frac{1}{2}\,m\,\omega_c^2\,y^2. \tag{23}$$
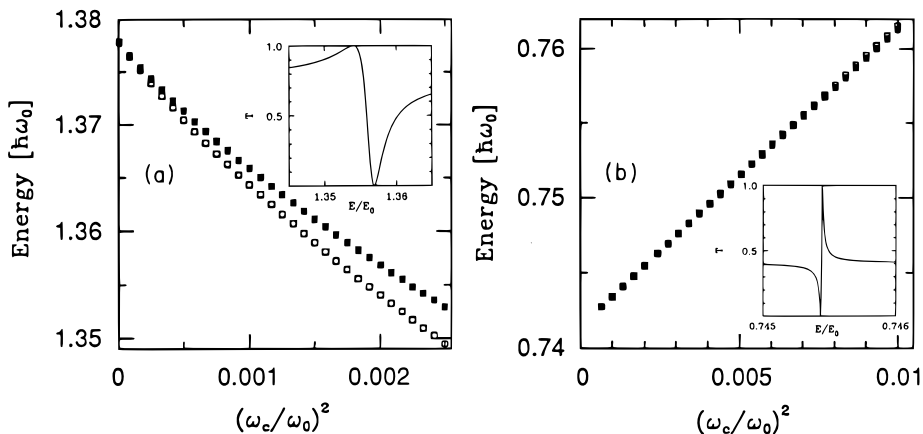
9

Figure 2: Positions of the transmission minimum (solid dots) and maximum (open dots) versus ω_c^2/ω_0^2 for resonances due to a bound state in (a) subband $n = 2$ and (b) $n = 3$. The system consists of a quantum wire with a rectangular well of length $L = 3.5\sqrt{\hbar/m\omega_0}$ and depth $U_0 = 2\hbar\omega_0$. The $n = 3$ resonance is much narrower than the one with $n = 2$, so minima and maxima are almost indistinguishable on the energy scale in (b). In both plots, the curves start out linearly in ω_c^2/ω_0^2, indicating a quadratic energy shift at small ω_c, although the coupled-channel model predicts an ω_c^4 law in case (b). Insets: the corresponding resonance lineshapes at $\omega_c^2/\omega_0^2 = 0.002$.

Due to the parity of the transverse harmonic oscillator eigenfunctions, at most one of the terms in this sum can contribute to the matrix elements $\hat{V}_{nl}$. In particular, one has

$$\hat{V}_{12} = \hat{V}_{21} = -\omega_c\sqrt{\frac{\hbar}{2m\omega_0}}\,p_x, \tag{24}$$

whereas the diagonal elements $\hat{V}_{11}$ and $\hat{V}_{22}$ simply yield a constant proportional to ω_c^2. Equation (24) shows why we needed to generalize the Feshbach approach to coupling operators that are not scalar potentials. Note that $\hat{V}_{12}$ satisfies the criterion of Appendix A, so that we might hope to apply the previous results to this case. This will be done by comparing the ω_c dependence of the resonance position as obtained from exact numerical calculations with that predicted by the approximation. First note that only matrix elements between transverse subbands that differ by exactly 1 in their mode index [like the one in Eq. (24)] have a linear dependence on ω_c. All others either vanish due to parity or go as ω_c^2.

A resonance occurs in our model system when the well potential $U(x)$ causes bound states to split off from a subband $n > 1$ which lie in the continuum of the lowest subband. The bound state becomes metastable when a magnetic field is switched on, so the resonance linewidth depends on ω_c. The same is true for the energy shifts Δ, δ and η. From their definitions in Eqs. (95), (96) and (105) it follows that $\Delta, \delta, \eta \propto \omega_c^2$ if the quasi-bound state occurs in subband $n = 2$, whereas $\Delta, \delta, \eta \propto \omega_c^4$ for resonances originating from higher subbands, $n \geq 3$. This conclusion holds irrespective of the number of intermediate closed channels we take into account [29], because that simply

10

adds to $\hat{V}_{1n}$ terms containing two or more matrix elements, cf. Eq. (20). It is in fact necessary to include more than two subbands in the calculation because a bound state in subband $n = 3$ cannot couple at all to the propagating subband $n = 1$ if only these two channels are taken into account. But a resonance *does* arise in this case [9], see inset to Fig. 2 (b). The numerical results show that the $n = 3$ resonance is narrower than the one arising from a bound state in $n = 2$, which is consistent with the weaker coupling expected for $n = 3$. We consider here a structure of the same dimensions as in Ref. [9], and record the resonance position as a function of ω_c. In Fig. 2 (a), the quadratic law is confirmed for the $n = 2$ resonance of Fig. 3 in Ref. [9]. However, the $n = 3$ resonance does *not* shift with ω_c^4, as seen in Fig. 2 (b). If we do not truncate the coupled-channel equations, Eq. (6), but instead take intermediate channels into account by substitutions of the kind shown in Eq. (20), then all the formal steps in the Feshbach treatment are valid for the present example, *except* the the ansatz Eq. (12). The notion of the metastable state wavefunction as a slightly modified bound state wavefunction cannot lead to the correct solution here. The reason is that the magnetic field not only couples bound state and continuum, but modifies the continuum itself. The special property of $\hat{V}^{xy}$ in Eq. (23) is that it is not localized in the x-direction. The propagating subband far away from the scattering region has a transverse wavefunction that is no longer given by $\phi_n(y)$, but by a *shifted* harmonic oscillator function. To construct the correct wavefunction in the asymptotic region, one therefore needs a superposition of different ϕ_n, which means that their respective coefficients $\psi_n(x)$ in the expansion of Eq. (5) cannot in general decay with $|x|$. In particular, the ansatz $\psi_n = A\,\Phi_0$ for a quasibound state in subband n is not justified when $\omega_c \neq 0$, unless the admixture of ϕ_n in the true transverse wavefunction of the propagating subband happens to be negligible.

The example treated here matches the qualitative description given at the beginning of this Section – quasibound states in one subband lying in the continuum of a propagating subband – but cannot be modeled with the present approach. Still, the resonance lineshapes found numerically are of the Fano type, and exact transmission zeros persist, as do the points of unit transmission expected due to inversion symmetry. The explanation for this will be given in the next Section. One might ask whether all resonances in Q1D systems can be described in terms of quasibound states splitting off from non-propagating subbands. The answer is negative; examples are the resonant stub structure [7] and the Aharonov-Bohm ring with two leads attached [2]. In both cases one finds resonances of the Fano lineshape even when the motion between all junctions occuring in the geometry is treated as purely one-dimensional [30], i.e., no subband structure is taken into account. Those resonances display zero and unit transmission if the system is symmetric, even though the derivation that led us to this phenomenon above does not apply. A more general treatment is thus called for, and that is the task we take up now.

3. S-MATRIX APPROACH

The Feshbach approach enabled us to relate all the parameters determining the resonance lineshape and position to properties of the original Hamiltonian. The linewidth Γ is

obviously a measure of the coupling that renders the originally bound state metastable (note that in this paper Γ is the half-width of the Breit-Wigner resonance, whereas sometimes Γ is used to denote the full width). As is well-known for the case of Breit-Wigner resonances, $2\Gamma/\hbar$ is the decay rate of this quasibound state [31]. Instead of starting from a bound state and introducing a coupling to the continuum, we could equivalently start with a metastable state whose decay rate is given by 2Γ, and derive the resulting transmission behavior. This procedure is in fact more general because it makes no assumptiuons about the number of subbands participating in the metastable state. We shall see in this section that the results derived previouly are confirmed and extended if we make use of the relation between quasibound states and poles of the S-matrix, established in subsection 3.1.

The S-matrix relates the amplitudes of the incomig and outgoing waves in all the subbands of all the leads. If the total number of subbands in all leads is N, we can specify the incoming and outgoing amplitudes by complex N-vectors $\mathbf{I}$ and $\mathbf{O}$ and write

$$\mathbf{O} = S\,\mathbf{I}, \tag{25}$$

where the $N \times N$ matrix S is unitary at real energies E, due to current conservation. We have to address here a point that might cause confusion. If S is the unit matrix, that does not imply the absence of any scattering as it does in conventional scattering theory. Instead, $S = 1$ corresponds to perfect reflection of all incoming waves, without intersubband transitions. The representation in Eq. (25) is convenient for extracting measurable quantities from S when dealing with multilead structures. The quantities of interest in a multiprobe experiment are the conductance coefficients relating the current in a given lead to the voltages of all the attached reservoirs. The Landauer-Büttiker formula [1] allows us to calculate these coefficients from the matrix elements of S as defined above.

In Subsection 3.1 we briefly review the connection between quasi-bound states and resonances, and show that the standard approach of multichannel scattering theory in the absence of symmetries does not correctly reproduce the statements derived in Section 2 because one arrives at a lineshape expression that contains too many parameters. This raises the question of whether S-matrix theory intrinsically provides too little information to make strong predictions, e.g. about the existence of transmission zeros. To prove that this is not so, we start by considering scattering geometries with symmetries that reduce the number of free parameters in the problem. In Subsection 3.2 we discuss Q1D structures with a discrete rotation symmetry and derive a multiprobe lineshape formula. The differences between the multilead system and a purely two-dimensional problem will be discussed in Subsection 3.3. In Subsection 3.4, we proceed to the most general multisubband and multilead structures. Finally, the special case of multisubband two-probe structures is addressed in Subsection 3.5.

3.1. POLES OF THE S-MATRIX

A resonance that arises from the coupling between a bound state and a continuum can be associated with a metastable state that has an exponentially decaying time depen-

dence. Since that time dependence is $e^{-iEt/\hbar}$ for time-independent Hamiltonians, such a quasibound state is a solution of the Schrödinger equation for complex $\bar{E} \equiv E_R - i\Gamma$ with $\Gamma > 0$. At that $\bar{E}$, a set of outgoing waves with exponential growth in the leads exists in the absence of any incoming waves [32] (referred to in nuclear physics as Gamow states [33]). This means that the determinant of S^{-1} vanishes there, and consequently at least one eigenvalue of S^{-1} must be zero. The corresponding eigenvalue λ_j of S thus has a pole at $\bar{E}$. This pole will appear in the matrix elements of S, too, if they contain contributions from this eigenvalue. Therefore, one can speak of a pole of the matrix S. This is precisely the phenomenon which occurred in Section 2, as can be seen from the resonance denominators in Eqs. (102) and (107). Thus, the results of that section are a special case of the conclusions to be derived later.

For real E, λ_j is unimodular and can be written as $\lambda_j \equiv e^{2i\theta_j}$ with θ_j real. The linear approximation to λ_j in the complex plane near resonance that maps real energies E onto the unit circle and has a pole at $\bar{E}$ is [34]

$$\lambda_j(E) \approx e^{2i\bar{\theta}_j} \frac{E - \bar{E}^*}{E - \bar{E}} \equiv e^{2i\bar{\theta}_j} e^{-2i\theta} \tag{26}$$

where θ is the phase angle of $E - \bar{E}$ (E real),

$$\tan\theta = \frac{\Gamma}{E - E_R}, \tag{27}$$

and $\bar{\theta}_j$ is an arbitrary phase that we assume to be slowly varying with E. This leads to

$$\theta_j \approx \bar{\theta}_j - \arctan\frac{\Gamma}{E - E_R} \tag{28}$$

so that we now have the energy dependence of the resonant eigenvalue λ_j in terms of E_R, Γ and the phase $\bar{\theta}_j$. We assume that the zero of $\det(S^{-1})$ is a simple one so that only a single λ_j is resonant and all others vary slowly with E.

The problem is how to deduce the reflection and transmission coefficients from a knowledge of just the eigenvalues of S. This is possible only if the number of independent matrix elements in S does not exceed its dimension. Being an $N \times N$ unitary matrix, S in general has N^2 independent parameters, so that it is not uniquely determined by its N eigenvalues. Another $N(N-1)$ parameters must be implicit in the transformation that diagonalizes S, unless there are unitary or antiunitary (time-reversal) symmetries in the problem that imply additional relations between elements of S. If this is not the case, we are faced with a situation familiar from the theory of multichannel scattering. The approach commonly taken there [35, 34] is to make the ansatz that each S-matrix element S_{mn} will itself exhibit a resonance denominator as in Eq. (26):

$$S_{mn} = S_{mn}^{bg} - i\frac{\gamma_m \delta_n^*}{E - E_R + i\Gamma}, \tag{29}$$

where S^{bg} is the background scattering matrix in the absence of the resonance and $\vec{\gamma}$, $\vec{\delta}$ are complex vectors which must satisfy $\vec{\gamma} = S^{bg}\vec{\delta}$ and $|\vec{\gamma}|^2 = |\vec{\delta}|^2 = 2\Gamma$ so that S is

unitary. The individual $|\gamma_m|^2$, $|\delta_n|^2$ are then interpreted as partial widths for leaving and entering the resonance [34]. However, Eq. (29) contains more than N^2 parameters since S^{bg} is itself a general unitary matrix. It turns out that the parameterization in Eq. (29) underconstrains the S-matrix, allowing lineshapes that cannot arise in reality from a nondegenerate, simple and isolated resonance pole. For instance, according to Eq. (29) a 2×2 S-matrix with $S_{12}^{bg} = S_{21}^{bg} = 1$ gives rise to a transmission S_{12} that never goes to zero if $|\gamma_1|^2 \neq \Gamma$. To see this, note first that $\delta_2 = \gamma_1$ so that $\gamma_1 \delta_2^* = |\gamma_1|^2$. According to the definition in Eq. (27),

$$\frac{1}{E - E_R + i\Gamma} = \frac{1}{\sqrt{(E - E_R)^2 + \Gamma^2}} \, e^{-i\theta}, \tag{30}$$

so that we can write

$$S_{12} = 1 + \frac{|\gamma_1|^2}{2\Gamma} \left(e^{-2i\theta} - 1 \right). \tag{31}$$

Across the resonance, 2θ varies by 2π, and $|S_{12}|^2 = 0$ can only occur if $|\gamma_1|^2 = \Gamma$. However we show below that transmission zeros are present in the most general two-probe (2×2) Q1D resonant S-matrix. A simplified version of Eq. (29) which assumes the background S-matrix to be diagonal is often used[35] and in particular was employed by Büttiker [21] to derive the lineshape of resonances in Q1D structures with time-reversal symmetry. With this further approximation we no longer have too many parameters, but too few of them. The results in that case are consistent with our work, but one always arrives at symmetric resonance lineshapes. This is all that is needed in the resonant tunneling regime on which Ref. [21] focuses, because we have already seen in Section 2 that the Breit-Wigner lineshape results when the nonresonant transmission is negligible. But as pointed out in the Introduction, we wish to understand the implications of interference between resonant and nonresonant scattering in the general case.

3.2. N-FOLD ROTATION SYMMETRY

Low-dimensional systems always break full rotational symmetry because leads are attached to the sample. However, we can perform the analog of the preceding partial wave analysis if the scattering geometry still is invariant under a *finite* rotation group. The inversion symmetry considered in Section 2 for the two-probe case is a special case of this, the rotation group being C_2. The fourfold symmetry of the cross junction has been used by Schult *et al.* [4] to perform a numerical phase shift analysis of the resonances found in that system. There is one complication that does not arise in purely two-dimensional systems, namely the possibility of more than one propagating subband in the leads. In that case, symmetry alone does not suffice to diagonalize the S-matrix because it is impossible to transform different subbands of one lead into each other by means of a symmetry operation. Therefore we first consider the case where each lead supports exactly one propagating subband. Each component of the amplitude vectors $\mathbf{I}$ and $\mathbf{O}$ then refers to a different lead. For a general N-lead geometry in the single-subband regime with symmetry group C_N, there are N one-dimensional irreducible representations with

characters

$$\chi^{(q)}(p) = e^{-2\pi i p q / N}, \qquad (p,\, q = 1, \dots N). \tag{32}$$

Here, p labels the elements R_p of the rotation group, and q enumerates the representations. From the N degenerate scattering states corresponding to an incoming electron in exactly one of the leads, we can form symmetrized eigenfunctions by taking the incoming waves as $\mathbf{I}^{(q)}$ with components

$$I_p^{(q)} = \frac{1}{\sqrt{N}} \chi^{(q)}(p)^*. \tag{33}$$

For any rotation R_p, one then has $R_p \, \mathbf{I}^{(q)} = \chi^{(q)}(p) \, \mathbf{I}^{(q)}$. But since R_p leaves the system invariant, a rotation of the incoming wave amplitudes $R_p \, \mathbf{I}$ leads to outgoing waves $R_p \, \mathbf{O}$. For the symmetrized waves this means

$$R_p \, \mathbf{O} = S \, R_p \, \mathbf{I}^{(q)} = \chi^{(q)}(p) \, S \, \mathbf{I}^{(q)} = \chi^{(q)}(p) \, \mathbf{O}. \tag{34}$$

This implies that $\mathbf{O}$ transforms under the rotations in the same way as $\mathbf{I}^{(q)}$. Since the representations are one-dimensional, it follows that $\mathbf{O} \propto \mathbf{I}^{(q)}$, so that the $\mathbf{I}^{(q)}$ are an eigenbasis of S. The unitary transformation relating the matrix elements of S between incoming and outgoing waves in leads m and n to the diagonal elements λ_j is then given by

$$
\begin{aligned}
S_{mn} &= \frac{1}{N} \sum_{j=1}^{N} \chi^{(m)}(j)^* \, \lambda_j \, \chi^{(n)}(j) \tag{35}\\
&= \frac{1}{N} \sum_{j=1}^{N} e^{2i\theta_j} \, e^{2\pi i (m-n) j / N}. \tag{36}
\end{aligned}
$$

This shows that S_{mn} only depends on the angle $2\pi(m-n)/N$ between leads m and n, and it is an exact expression for the multiprobe scattering amplitude. Now assume without loss of generality that θ_N is the resonant eigenphase while all other θ_j are slowly varying with energy. Then we abbreviate the sum over the nonresonant eigenvalues by

$$\sum_{j=1}^{N-1} e^{2i\theta_j} \, e^{2\pi i (m-n) j / N} \equiv \rho_{mn} \, e^{2i\tilde{\theta}_{mn}} \tag{37}$$

where clearly $\rho \leq N - 1$. With this one obtains for the scattering probabilities (which determine the conductance coefficients)

$$|S_{mn}|^2 = \left(\frac{\rho_{mn} - 1}{N} \right)^2 + 4 \frac{\rho_{mn}}{N^2} \sin^2\!\left(\tilde{\theta}_{mn} - \frac{\pi}{2} - \theta_N \right). \tag{38}$$

The factor $\sin^2(\dots)$ in the above expression in fact leads to the Fano lineshape, as we now show. Denote the slowly-varying phases by $\bar{\theta}$ and use Eq. (28) for θ_N. Then

$$
\begin{aligned}
\sin^2(\bar{\theta} + \theta_N) &= \sin^2\!\left[\bar{\theta} + \arctan \frac{\Gamma}{E - E_R} \right] \tag{39}\\
&= \sin^2(\bar{\theta}) \, \frac{\left[E - E_R + \Gamma \cot \bar{\theta} \right]^2}{(E - E_R)^2 + \Gamma^2} \tag{40}
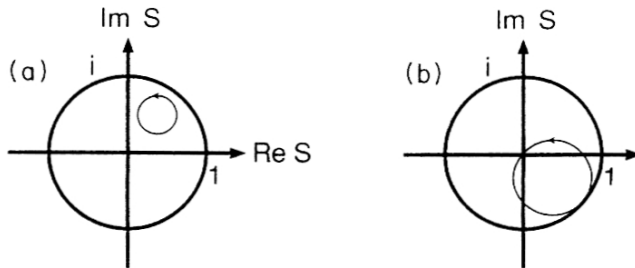\end{aligned}
$$

15

Figure 3: Variation of the S matrix elements in the complex plane as the resonace is crossed for two symmetric structures in the single-subband regime: (a) four-probe, (b) two-probe geometry. All S_{mn} trace out a circle (thin line) of radius $1/N$ lying entirely inside the unit circle (bold line). As shown in (b), the case $N = 2$ is special because all S_{mn} must describe circles that go through zero and unit modulus.

The factor $\sin^2 \bar{\theta}$ is just the value that $\sin^2(\bar{\theta} + \theta_N)$ would assume in the absence of any resonant contribution to the phase shift. The resonant behavior is described entirely by the second factor, which takes on the form of the Fano function if we set $\epsilon = (E - E_R)/\Gamma$ and $q = \cot \bar{\theta}$. We see that the asymmetry parameter in these units is again solely determined by the backgound phase shift. As noted in Section 1 below Eq. (2), the Breit-Wigner peak arises for negligible nonresonant scattering, $\sin^2 \bar{\theta} = 0$. Equation (38) implies that the effect of a resonance on any matrix element of S decreases as the number of leads, N, increases. More precisely, we can deduce

$$\left| \frac{\rho_{mn} - 1}{N} \right| \leq |S_{mn}| \leq \left| \frac{\rho_{mn} + 1}{N} \right|. \tag{41}$$

Thus, $|S_{mn}|$ varies exactly by $2/N$ if $\rho_{mn} \geq 1$, and by $2\rho_{mn}/N$ otherwise. The maximum variation in $|S_{mn}|$ is therefore $2/N$, and $|S_{mn}|^2$ varies by no more than $4(N - 1)/N^2$. The latter is stricly less than unity for $N > 2$, i.e. the transmission probabilities *cannot* assume all values allowed by unitarity unless $N = 2$. On the other hand, both zero and unit transmission are reached on resonance *if $N = 2$*. The reason is that $N = 2$ implies $\rho_{mn} = 1$, which is the necessary and sufficient condition for a zero in $|S_{mn}|^2$ because it makes the first term in Eq. (38) vanish. In that case we get

$$|S_{mn}|^2 = \begin{cases} \frac{4}{N^2} \sin^2(\theta_N - \theta_1) & (m \neq n) \\ 1 - 4\frac{N-1}{N^2} \sin^2(\theta_N - \theta_1) & (m = n) \end{cases} \tag{42}$$

which varies by unity for $N = 2$. We still get this expression for $N > 2$ provided that $\rho_{mn} = 1$ for $m \neq n$. This occurs when all the nonresonant eigenphases are the same:

$$\theta_1 = \theta_2 = \ldots = \theta_{N-1}. \tag{43}$$

The special role of $N = 2$ is illustrated in Fig. 3.

The general lineshape given by Eq. (38) has the Fano form superimposed on a slowly varying baseline, cf. Eq. (39). The transmission for $N = 2$ can be written using the

definition Eq. (28) as

$$T = |S_{21}|^2 = |t^{bg}|^2 \frac{(E - E_R + \delta)^2}{(E - E_R)^2 + \Gamma^2}, \tag{44}$$

where we have identified

$$|t^{bg}|^2 = \sin^2(\bar{\theta}_1 - \bar{\theta}_2) \tag{45}$$

as the (slowly-varying) transmission in the absence of the resonance, and introduced the energy shift

$$\delta = \Gamma \cot(\bar{\theta}_1 - \bar{\theta}_2). \tag{46}$$

This is the Fano lineshape, Eq. (1), with $\epsilon = (E - E_R)/\Gamma$ and $q = \delta/\Gamma = \cot(\bar{\theta}_1 - \bar{\theta}_2)$. From Eq. (36) with $N = 2$, we can also conclude $S_{11} = S_{22}$, $S_{12} = S_{21}$ and

$$i \frac{S_{11}}{S_{21}} = \cot(\theta_2 - \theta_1). \tag{47}$$

This relation also holds in the absence of any resonances, and in particular for the nonresonant S-matrix S^{bg} with $\theta_1 = \bar{\theta}_1$. This allows us to write for the asymmetry parameter

$$q = \frac{\delta}{\Gamma} = \cot(\theta_2 - \bar{\theta}) = i \frac{r^{bg}}{t^{bg}}, \tag{48}$$

where $r^{bg} = S_{11}^{bg}$ and $t^{bg} = S_{21}^{bg}$. Whereas Eq. (17) only determined the magnitude of q, this expression gives the sign, too.

We have thus provided a generalization of the result derived in Subsection 2.2 without any assumptions about the mechanism creating the resonance. These considerations are also valid if a homogenous magnetic field is applied perpendicular to the plane of the structure, because that has no effect on the rotation symmetries. The quantum wire structure with magnetic field discussed in Subsection 2.3 can therefore be described in the present formalism.

3.3. COMPARISON BETWEEN CONTINUOUS AND DISCRETE SYMMETRIES

As is to be expected, there is a strong formal similarity between the systems with continuous and discrete rotational symmetries, respectively. The S-matrix element in Eq. (36) can be rewritten as

$$S_{mn} - \delta_{mn} = \frac{2i}{N} \sum_{j=1}^{N} e^{i\theta_j} \sin\theta_j \, e^{2\pi i(m-n)j/N}. \tag{49}$$

Compare this to the scattering amplitude $f(\phi)$ in a rotationally invariant two-dimensional system (where ϕ is the angle with the beam direction). Since $f(\phi)$ is extracted from the asymptotic form of the scattering state by subtracting out the unscattered plane wave

component (leaving only the radial outgoing wave) it is related to matrix elements of $S - 1$. One finds for particles with momentum p

$$f(\phi) = \sqrt{\frac{2\hbar}{\pi p}} \sum_j e^{i\theta_j} \sin\theta_j \, e^{iq\phi} \tag{50}$$

where the eigenphases θ_j now have the interpretation of phase shifts in angular momentum channel j. Except for the prefactors in the definition of the scattering amplitude, Eqs. (50) and (49) are identical in form. In particular, one can obtain the 2D limit from the Q1D expression when $N \to \infty$.

However, the scattering properties of a Q1D structure are measured in a different way than those of a purely 2D system. Whereas the latter is characterized by cross sections, the former requires us to determine the conductance coefficients g_{mn}. The differential cross section is obtained from $f(\phi)$ through

$$\frac{d\sigma}{d\phi} = |f(\phi)|^2 = \frac{2\hbar}{\pi p} \sum_q \sum_r e^{i(\theta_q - \theta_r)} \sin\theta_q \sin\theta_r \, e^{i(q-r)\phi}. \tag{51}$$

In contrast, the conductance coefficients are *not* related to the absolute square of Eq. (49), but instead to $|S_{mn}|^2$ directly. These differ only for $m = n$, but this difference has physical consequences.

While S must account for all of the incident flux, $f(\phi)$ only represents the scattered portion of the incident flux. Flux conservation in two dimensions is satisfied because the radially outgoing flux measured by the total cross section σ is canceled by the interference terms between the scattered radial and unscattered plane wave, which is just the content of the optical theorem, $\sigma \propto \operatorname{Im} f(0)$ (since this interference is important only in the forward direction). On the other hand, flux conservation in Q1D simply means that $T \equiv 1 - |S_{nn}|^2$ is equal to the total transmission. Both T and the total cross section vanish when $S = 1$. The similarity goes further, in that the two-dimensional expression

$$\sigma = \frac{4\hbar}{p} \sum_j \sin^2\theta_j. \tag{52}$$

predicts a zero in σ on resonance whenever the phase shifts in all nonresonant channels are zero or multiples of π; under the same conditions, Eq. (42) yields a zero in the total transmission, *not* the reflection (except for the case $N = 2$ where both occurs). But one also observes that T goes to zero on resonance even if the nonresonant eigenphases (modulo π) are *not* zero, as long as they are all equal. This difference is caused by the way in which the background phase shifts enter into σ and T, respectively. In Eq. (38), $\tilde{\theta}_{mn}$ contains all nonresonant phase shifts whereas the partial cross sections in Eq. (52) only contain a single eigenphase. *This implies that the asymmetry of the resonance lineshape in two dimensions gives us information about a single background phase shift, whereas the asymmetry in Q1D is influenced by all background phases simultaneously.* In other words, channels with different symmetry labels do not interfere in the total cross section, but do interfere in the total transmission. As a corollary, the $N \to \infty$ limit of

18

the total transmission T cannot be directly identified with the total cross section of a system with continuous symmetry. This can also be seen from Eq. (38) for the reflection $|S_{nn}|^2$, which shows no resonant variation at all if we let $N \to \infty$.

3.4. MULTISUBBAND, MULTILEAD STRUCTURES WITHOUT SYMMETRIES

For the multilead structure with discrete rotation symmetry and a single subband per lead, we were able to derive the inequality (41). As a consequence, the resonant variation ΔT of the total transmission from one lead into all the others satisfies

$$\Delta T \le 4(N-1)/N^2. \tag{53}$$

In the absence of symmetries, we no longer know the transformation that brings S to the diagonal form Λ,

$$U \, S \, U^\dagger = \Lambda, \tag{54}$$

unless we solve the scattering problem itself. Therefore, the constraints on ΔT will become weaker.

For a two-probe structure with time reversal symmetry, various authors [21, 22, 23] showed for the special case of Breit-Wigner resonances in the resonant tunneling regime that the conductance cannot vary by more than e^2/h on resonance, *independently* of the number of propagating subbands per lead. Since the more general Fano lineshape occurs in the presence of significant background transmission, it is worth asking what the maximum conductance variation will be in this case. In particular, if complete destructive interference between resonant and background transmission could still occur even for a total background larger than unity, this would imply a resonant conductance variation that exceeds e^2/h according to the two-probe Landauer formula [1],

$$G = \frac{e^2}{h} \, T. \tag{55}$$

This equation relates the conductance G to the total transmission T. The generalization of this quantity to a structure with arbitrary number of subbands *and* leads is the transmission from all subbands of one lead into all the subbands of all other leads. We first want to prove the following *theorem*:

$$\Delta T \le 1 \tag{56}$$

independent of the number of subbands or leads in the structure, and independent of the nonresonant transmission. This means that complete destructive interference in T is impossible if the background is larger than one.

In terms of the S-matrix of dimension N as defined in Eq. (25), we can define the total transmission by assigning different labels to the subbands in the incoming and outgoing leads, respectively. Let a run over all the subbands in the incoming lead and b enumerate

all the subbands in all the other leads, so that all N subbands are indexed either by a or b. Then

$$T = \sum_{ab} |S_{ba}|^2. \tag{57}$$

According to Eq. (54), we can express S in terms of its eigenvalues,

$$S_{ba} = \sum_{j=1}^{N} U_{jb}^* \, \lambda_j \, U_{jb}. \tag{58}$$

Now assume without loss of generality λ_1 to be resonant so that its phase is given by Eq. (28),

$$\lambda_1 = e^{2i\bar{\theta}_1} \, e^{-2i\theta}. \tag{59}$$

Here, 2θ varies by 2π on resonance. The other eigenvalues are assumed constant and will be written as

$$\lambda_j = e^{2i\bar{\theta}_j}. \tag{60}$$

In order to compare with the ansatz in Eq. (29), we split off the resonant term in S_{ba} to obtain

$$S_{ba} = \sum_{j=1}^{N} U_{jb}^* \, e^{2i\bar{\theta}_j} \, U_{ja} + U_{1b}^* U_{1a} \left(e^{2i\bar{\theta}_1} \, e^{-2i\theta} - e^{2i\bar{\theta}_1} \right). \tag{61}$$

The first term is just the nonresonant transmission, S_{bl}^{bg}. Using Eq. (27), this can also be written as

$$S_{ba} = S_{ba}^{bg} - 2i\Gamma U_{1b}^* U_{1a} \, e^{2i\bar{\theta}_1} \, \frac{1}{E - E_R + i\Gamma}. \tag{62}$$

This has the same form as Eq. (29) but gives us an explicit expression for the partial decay width: one can set

$$\gamma_n = \delta_n^* = \sqrt{2\Gamma} \, e^{i\bar{\theta}_1} \, U_{1n}^*. \tag{63}$$

Clearly, this no longer contains too many independent parameters because we have simply reexpressed S in terms of its eigenvalues and eigenvectors. It is useful to define

$$A^2 \equiv \sum_a |U_{1a}|^2, \tag{64}$$

$$B^2 \equiv \sum_b |U_{1b}|^2$$

so that $A^2 + B^2 = 1$. Then $\Gamma_a \equiv 2\Gamma A^2$ is the partial decay rate of the quasibound state into the incoming lead, and similarly $\Gamma_b \equiv 2\Gamma B^2$ measures the decay into all other leads. Since $\Gamma = (\Gamma_a + \Gamma_b)/2$, we can also write

$$A^2 = \frac{\Gamma_a}{\Gamma_a + \Gamma_b}. \tag{65}$$

Returning to Eq. (61), the total resonant transmission becomes

$$T = \sum_{ab} |S_{ba}^{bg}|^2 + 4\sin^2\theta \sum_{ab} |U_{1b}|^2 |U_{1a}|^2$$

$$+ \left\{ \sum_{ab} S_{ba}^{bg} U_{1b} U_{1a}^* e^{-2i\bar{\theta}_1} \left(e^{2i\theta} - 1 \right) + \quad \text{c.c.} \right\}. \tag{66}$$

The first cross term (curly brackets) can be written more explicitly as

$$\sum_{ab} \sum_{j=1}^{N} U_{jb}^* e^{2i\bar{\theta}_j} U_{ja} U_{1b} U_{1a}^* e^{-2i\bar{\theta}_1} \left(e^{2i\theta} - 1 \right)$$

$$= \left(e^{2i\theta} - 1 \right) \sum_{ab} |U_{1b}|^2 |U_{1a}|^2 + e^{-2i\bar{\theta}_1} \left(e^{2i\theta} - 1 \right) \sum_{j=2}^{N} e^{2i\bar{\theta}_j} \sum_{ab} U_{jb}^* U_{1b} U_{ja} U_{1a}^*. \tag{67}$$

Now we note that the unitarity of the transformation U,

$$\sum_b U_{jb}^* U_{1b} + \sum_a U_{ja}^* U_{1a} = \delta_{j,1}, \tag{68}$$

implies for $j \neq 1$

$$\sum_b U_{jb}^* U_{1b} \sum_a U_{ja} U_{1a}^* = - \left| \sum_a U_{ja} U_{1a}^* \right|^2 \equiv -Q_j^2. \tag{69}$$

Using this and the definitions of A^2, B^2 in Eq. (67) and adding the complex conjugate, the cross terms in Eq. (66) now take the form

$$-4 A^2 B^2 \sin^2\theta$$

$$+4 \sum_{j=2}^{N} Q_j^2 \left[\sin^2(\theta + \bar{\theta}_j - \bar{\theta}_1) - \sin^2(\bar{\theta}_j - \bar{\theta}_1) \right]. \tag{70}$$

Substituting this into Eq. (66), the total transmission is now

$$T = \sum_{ab} |S_{ba}^{bg}|^2 - 4 \sum_{j=2}^{N} Q_j^2 \sin^2(\bar{\theta}_j - \bar{\theta}_1)$$

$$+4 \sum_{j=2}^{N} Q_j^2 \sin^2(\theta + \bar{\theta}_j - \bar{\theta}_1). \tag{71}$$

Using the definition of θ as in Eq. (39) we see that the last term is a superposition of Fano lineshapes, but in general with differing prefactors and asymmetry parameters. It can be shown that such a sum again yields a Fano function plus some constant. This is then added to the constant terms in Eq. (71). The question now is what the maximum

variation in T can be. As 2θ varies by 2π in Eq. (71), T shows the largest variation if and only if the nonresonant phase shifts satisfy

$$\sin^2(\bar{\theta}_j - \bar{\theta}_1) = C \tag{72}$$

for all $j \geq 2$ (with $Q_j \neq 0$). Then one can use the unitarity of U to derive

$$\sum_{j=2}^{N} Q_j^2 = A^2 B^2, \tag{73}$$

which leads to

$$
\begin{aligned}
T &= \sum_{ab} |S_{ba}^{bg}|^2 - 4A^2 B^2 \sin^2(\bar{\theta}_2 - \bar{\theta}_1) \\
&\quad + 4A^2 B^2 \sin^2(\theta + \bar{\theta}_2 - \bar{\theta}_1).
\end{aligned} \tag{74}
$$

Still assuming Eq. (72) is satisfied, some further algebra leads to the following result for the total background transmission:

$$T^{bg} = \sum_{ab} |S_{ba}^{bg}|^2 = 4A^2 B^2 \sin^2(\bar{\theta}_2 - \bar{\theta}_1). \tag{75}$$

This cancels the second term in Eq. (74). The total transmission therefore has the pure Fano lineshape and goes to zero at some energy:

$$T = 4A^2 B^2 \sin^2(\theta + \bar{\theta}_2 - \bar{\theta}_1). \tag{76}$$

This holds whenever the nonresonant eigenphases are such as to maximize the variation in T. The magnitude of this variation ΔT now still depends on $A^2 B^2$. Recalling the definitions in Eq. (64), we observe that $A^2 B^2 \leq 1/4$ and consequently $\Delta T \leq 1$. We have thus shown for the most general lineshape that the resonant transmission never varies by more than unity, independent of the number of subbands or leads.

The resonant tunneling transmission constitutes a special case of Eq. (76) because Eq. (72) automatically holds there: when the background transmission vanishes, $S_{ba}^{bg} = 0$ for all a, b, so that the cross terms in Eq. (66) actually have to vanish. Thus Eq. (70) must yield zero, which requires that Eq. (72) hold with $C = 0$. We therefore can use Eq. (76) with $\bar{\theta}_2 - \bar{\theta}_1 = 0$ and obtain the Breit-Wigner lineshape for the total transmission, independently of the number of subbands or leads,

$$T = 4 A^2 B^2 \frac{\Gamma^2}{(E - E_R)^2 + \Gamma^2}. \tag{77}$$

A further implication of the above calculation is that *if $T^{bg} > 1$ then Eq. (75) cannot be true, so that Eq. (72) must be violated. But then the maximum variation $\Delta T = 1$ is impossible.* This happens, e.g., in quantum point contacts above the second conductance step. Whereas resonances on the first quantized plateau display unit variation in T as shown in Ref. [19], this cannot occur on higher plateaus. It is worth emphasizing this because a naive generalization of the two-channel result of Ref. [19] would state that antiresonances on the n-th conductance plateau drop to a minimum value of $(n - 1)$ times the conductance quantum.

3.5. MULTISUBBAND TWO-PROBE STRUCTURES

The quantum constriction is a two-probe structure, and we now specialize the discussion to such systems to explore if further statements can be made when there are only two leads, but arbitrarily many subbands. In this case A^2 and B^2 measure the decay probabilities of the quasibound state into the left and right lead, respectively. A strong statement that has been proved in the resonant tunneling regime ($T^{bg} \to 0$) is that symmetric two-probe structures structures always exhibit $\Delta T = 1$ on resonance [21, 23]. This theorem is no longer valid in general when there is more than one propagating subband in the leads and nonresonant transmission is appreciable, because in that case one can have $T^{bg} > 1$ and the above discussion applies. In fact, as Eq. (71) allows Breit-Wigner lineshapes even if Eq. (72) does not hold [36], S-matrix theory *allows* Breit-Wigner lineshapes that do not vary by unity in symmetric systems. Whether there exist potentials that actually produce such resonances is an open question.

We do recover the resonant tunneling result, however, if the condition in Eq. (72) is satisfied. To see this, note that if the system has inversion or reflection symmetry, the rows of U (being eigenvectors of S) satisfy

$$U_{ja} = \pm U_{jb} \quad (j = 1 \ldots N), \tag{78}$$

where a and b refer to the same subband in the left and right lead, respectively. This implies $A^2 = B^2 = 1/2$ and thus $\Delta T = 1$ in Eq. (76). We note two special cases of Eq. (72). First, the resonant tunneling limit. One can use Eq. (65) to write Eq. (77) in the form known from the asymmetric double barrier [21, 37],

$$T = \frac{\Gamma_l \, \Gamma_r}{(E - E_R)^2 + (\Gamma_l + \Gamma_r)^2/4}. \tag{79}$$

Here, we have identified $l \equiv a$ and $r \equiv b$ since Γ_l, Γ_r are simply the partial decay rates into the left and right lead, respectively.

The resonant tunneling structure, however, is not the only example in which Eq. (72) is satisfied. Another special case in which Eq. (76) must hold is the two-probe structure with only one propagating subband per lead. There, the sums over j in Eq. (71) contain just a single term because $N = 2$. This confirms our result in Section 2 that the Fano lineshape with exact transmission zeros will occur invariably if the S-matrix is of dimension $N = 2$, but unit transmission need not be reached on resonance if there are no symmetries.

4. QUASI-ONE-DIMENSIONAL MODEL SYSTEMS

One result derived in the previous section is that the Fano function is the generic resonance lineshape for any S-matrix of dimension 2, under the condition that the only rapid variation in energy occurs in one of the eigenphases. The distinction between quasi- and purely one-dimensional systems did not enter that discussion since a 2×2 S-matrix can describe both cases.

To understand why the Fano function is never seen in purely one-dimensional scattering, we have to come back to the general physical differences between Q1D and strictly one dimension. In the latter case, exemplified by a double-barrier resonant tunneling device [31], background transmission $|t^{bg}|^2$ and decay rate Γ of the metastable state are not independent. Well-defined resonances with small Γ require low background transmission, which simply gives the Breit-Wigner lineshape. In a Q1D system, on the other hand, an electron entering the region where the quasi-bound state is localized does not necessarily enter that state itself, because the existence of a second scattering channel allows resonant and nonresonant transmission to occur in parallel as two distinct processes. The background transmission can still be large even if the coupling to the quasi-bound level (which determines Γ) is small, (e.g. due to approximate symmetry).

Since the energy shifts δ in Eqs. (109), (44) are proportional to Γ, the asymmetry parameter q defining the lineshape is actually *independent* of Γ. If Γ can be varied while $|t^{bg}|^2$ is roughly constant across resonance, a series of Fano lineshapes will be obtained which can be collapsed onto a curve characterized by a single asymmetry parameter q by rescaling the energy axis. This scaling property may be tested for the first time in transport experiments.

In addition to the quantum wire structure studied in Ref. [9] and discussed in Subsection 2.3, we have explored two different systems which might exhibit Fano resonances when appropriately perturbed to create a quasi-bound level in the continuum. Since we desire external control over the resonance lifetime, it is necessary to minimize broadening due to inelastic scattering or disorder. The aim must therefore be to fabricate such structures with atomic precision, which has not yet been achieved with quantum wires suitable for transport measurements [38]. We thus consider Fano resonances in a three-dimensional heterostructure with a tilted magnetic field, and in a two-dimensional electron gas with an in-plane magnetic field. These systems can be realized purely by crystal growth (e.g., molecular beam epitaxy). Furthermore, they can be mapped onto the quantum wire problem already solved in Ref. [9] and discussed above in Subsection 2.3.

4.1. QUANTUM WELL IN TILTED MAGNETIC FIELD

One way to achieve ideal parabolic quantum wire confinement is by applying a homogenous magnetic field B to a three-dimensional free electron gas. The motion along the field lines is free, whereas the transverse orbits are quantized into Landau levels (LL) which in the Landau gauge yield harmonic oscillator wavefunctions. The calculation is described in Ref. [18]. Here, we describe the proposed experiment and present the predicted results.

Consider a layered structure of the type shown in Fig. 4). The emitter and collector regions are degenerately doped, the spacer layers are of the same composition as the contacts but undoped. the central part consists of a single undoped well with a band gap that is lower than in the contacts. In the region made up of the well and spacer layers transport is assumed to be ballistic. There will be some band bending at the well interfaces, but we neglect this effect in the numerical calculation because it only affects
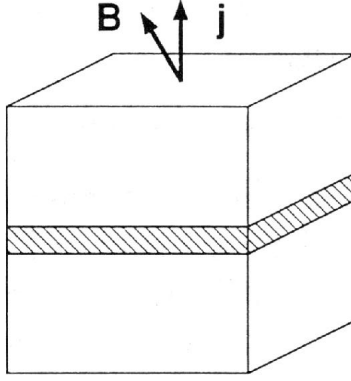
Figure 4: A finite quantum well (shaded region) in a magnetic field **B** that is tilted with respect to the vertical direction **x**. We measure the current across the well as a function of B. The undoped well is separated from the doped contacts by undoped spacer layers of the same composition as the contacts.

the exact resonance energies but not their shape. Since the structure contains no tunnel barriers, it is possible to drive a current without large voltage drop. We can therefore use the linear response approximation in which the net current is determined only by the transmission at the Fermi energy E_F. At a given carrier concentration in the contacts (determined by the doping), we can vary E_F by changing the magnetic field. Since the LL degeneracy is proportional to B, one can make E_F approach the the bottom of the lowest LL, E_1, by increasing B. At the same time, E_1 itself increases with B so that E_F will eventually be pulled up together with E_1. The calculation has to include the effect of spin splitting, which is done in Appendix C. The result for E_F as a function of B is shown in the inset to Fig. 5.

The scattering problem at E_F is described by the Hamiltonian

$$H = \frac{1}{2m} \left[(p_x - m\,\omega_z\,y)^2 + p_y^2 + (p_z + m\,\omega_x\,y)^2 \right] + U(x) \pm \frac{1}{2} g^* \mu_B B \qquad (80)$$

where we defined

$$\omega_z \equiv \frac{eB_z}{mc}, \qquad \omega_x \equiv \frac{eB_x}{mc} \qquad (81)$$

and chose the gauge $\mathbf{A} = -B_z\,y\,\hat{\mathbf{x}} + B_x\,y\,\hat{\mathbf{z}}$ to describe the tilted magnetic field $\mathbf{B} = B_x\,\hat{\mathbf{x}} + B_z\,\hat{\mathbf{z}}$. We denote by $U(x)$ the effective potential due to the conduction band modulation in the growth direction x. In the Zeeman term, we introduced the electronic g-factor g^* and the Bohr magneton, $\mu_B = e\hbar/2m_e c$, which involves the bare electron mass instead of the effective mass.

Since $[H, p_z] = 0$, we use the ansatz

$$\Psi(x, y, z) = \psi(x, y)\, e^{ik_z z} \qquad (82)$$

to obtain a two-dimensional Schrödinger equation for ψ. Comparison with Eq. (21) then shows that the resulting equation is precisely the Schrödinger equation of a parabolic
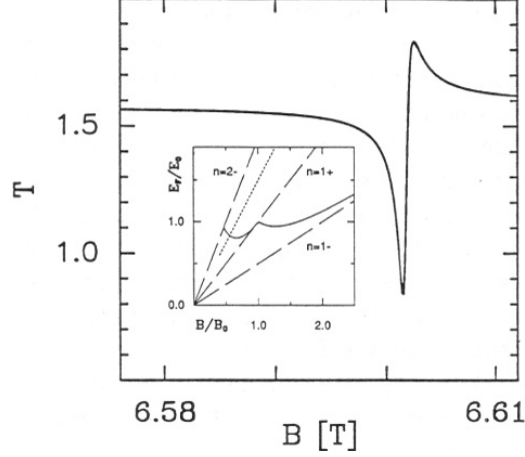
Figure 5: Transmission of a finite well as a function of magnetic field B in units of B_0. The tilt angles are $\sin\alpha = 0.12$ (dashed-dotted line), 0.1 (dashed line) and 0.08 (solid line). We chose a $Ga_xIn_{1-x}Sb$-$InSb$-$Ga_xIn_{1-x}Sb$ structure with well width $L = 25.9\,\mathrm{nm}$ and depth $V = 168\,\mathrm{meV}$. The large electronic g-factor and small effective mass of this compound combine to give $\eta \approx 1/3$, cf. [43]. *Inset:* Dependence of the Fermi energy on magnetic field B for $B > B_{\mathrm{th}}$. The straight dashed lines show the first ($n = 1\pm$) and second ($n = 2-$) spin-split Landau levels, and the dotted line represents the position of a resonance. The Fermi energy at B_0 is E_0.

quantum wire, shifted by $\frac{\hbar k_z}{m\omega_x}$, with a transverse magnetic field

$$\mathbf{B}' = \nabla \times (-B_z y\hat{\mathbf{x}}) = B_z\hat{\mathbf{z}}. \tag{83}$$

The current I flowing through a $y-z$ plane of the heterostructure (area A_{yz}) is obtained by integrating the x component of the current density over y and z, and summing over all k_z. The result is $I = A_{yz} B_x \frac{e}{hc} I'$, where I' is the current flowing through the equivalent quantum wire (this has no k_z dependence). In the following, we divide out the (known) degeneracy $= A_{yz} B_x \frac{e}{hc}$. If one assumes $U(x)$ to be a rectangular well, the transmission behavior of the heterostructure at low bias voltages in a tilted magnetic field follows straightforwardly from the numerical results of Refs. [9, 39].

The resulting transmission curves for the material system GaInSb-InSb-GaInSb and a particular choice of parameters are shown in Fig. 5 for a particular resonance at various small tilt angles α. The scaling property of the resonances (due to the independence of the asymmetry parameter q on tilt angle) is found to be well satisfied in this system [18]

4.2. TWO-DIMENSIONAL ELECTRON GAS WITH A GROOVE

Extremely high precision fabrication has been reported using the technique of cleaved edge overgrowth [40]. We propose to apply this method to create a two-dimensional electron gas (2DEG) divided by a thin straight groove in the conduction band bottom as shown in Fig. 6 (a).

The conductance is measured in linear transport from one side of the trench to the other, with a magnetic field $\mathbf{B}$ applied parallel to the trench. The Fermi energy E_F of
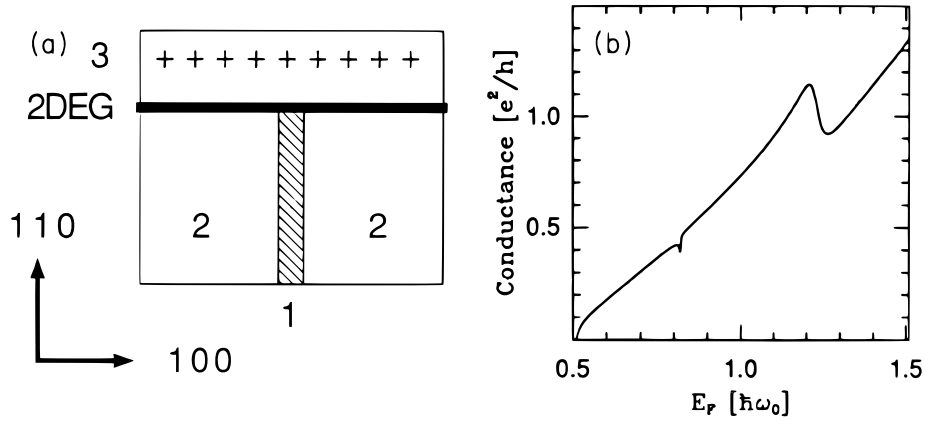
Figure 6: (a) A 2D electron gas forms at the interface between the n^+ doped high-band-gap region 3 and the undoped lower-gap material 1 with a quantum well. The band gaps must satisfy $E_g^1 < E_g^2 < E_g^3$. The effect of the well at the edge is to create a trench of lower effective potential in the 2D electron gas. A magnetic field B is applied parallel to the trench, i.e. pointing out of the page. (b) Conductance as a function of Fermi energy for a groove of length $L = 3.5\sqrt{\hbar/m\omega_0}$ and depth $U_0 = 2\,\hbar\omega_0$. The magnetic field is such that $\omega_c = 0.2\,\omega_0$.

the 2DEG is varied by means of additional gating, and the conductance as a function of E_F will be a convolution of a one-dimensional density of states and the Fano lineshape, with a decay width determined by the magnitude of $\mathbf{B}$. We neglect spin for the sake of clarity because it does not affect the proposed mechanism. If the 2DEG is in the xz-plane and the depression in the conduction band extends along the z-axis, we choose the Landau gauge $\mathbf{A} = -B\,y\,\hat{\mathbf{x}}$ to represent the field $\mathbf{B} = B\hat{\mathbf{z}}$. The trench potential is denoted by $U(x)$, and the vertical confinement potential creating the 2DEG subbands is $W(y)$. Since z is a cyclic coordinate in the Hamiltonian, we use the ansatz

$$\Psi(x,y,z) = \psi(x,y)\,e^{ik_z z} \tag{84}$$

to obtain a two-dimensional Schrödinger equation for ψ:

$$\left[\frac{1}{2m}\left\{(p_x - m\omega_c y)^2 + p_y^2\right\} + U(x) + W(y)\right]\psi(x,y) = \left(E - \frac{\hbar^2 k_z^2}{2m}\right)\psi(x,y). \tag{85}$$

Far away from the trench, where $U(x) = $ const, this is just the Schrödinger equation of a quantum wire with confining potential $W(y)$ in a transverse magnetic field, so $\psi(x,y)$ are the scattering states of this wire at energy $E' = E - \frac{\hbar^2 k_z^2}{2m}$. This means the y motion is quantized into modes (namely the subbands of the 2DEG) whereas one has reflected and transmitted plane waves in the x direction. In the absence of a magnetic field, x and y degrees of freedom are decoupled. This situation is again very similar to Eq. (21) if we specialize to a harmonic confinement, $W(y) = \frac{1}{2}m\omega_0^2 y^2$, except for the fact that k_z no longer labels degenerate eigenstates and thus appears in the dispersion relation.

27

If we solve Eq. (85) to obtain the transmission probabilities $T(E')$ across the potential well $V(x)$, then the conductance is

$$G = \frac{e^2}{h} \int\limits_0^{E_{\max}} dE\, g(E)\, T(E_F - E), \qquad (86)$$

where $E_{\max} = E_F - \hbar\omega_0/2$, and $g(E) = \frac{L_z}{2\pi}\sqrt{\frac{2m}{\hbar^2 E}}$ is the one-dimensional density of states which is peaked at $E = 0$. In Fig. (6) (b) we plot the resulting transmission for a structure with the same values of ω_0, L and U_0 as in the models discussed above. The asymmetries are still recognizable although the original Fano lineshape does not occur here. In particular, one can decide from the convoluted lineshape if the corresponding Fano resonance has a positive or negative asymmetry parameter: if the minimum in T occurs for lower E than the maximum, then G also shows a dip before the bump.

If G is measured as a function of E_F over a sufficiently wide range, then the convolution in Eq. (86) can be unfolded by Laplace transformation to get back $T(E)$.

5. CONCLUSION

We have attempted to shed light on the general properties of resonance lineshapes in systems where the asymptotic motion of the scattered particle is confined. The Feshbach approach was applied to scattering in a quantum wire without time reversal invariance and provides microscopic expressions for all lineshape parameters. In agreement with previous work, it predicts that there is always a transmission zero on resonance whereas a reflection zero is a consequence of additional symmetries. To reconcile this result with the more globally valid S-matrix formalism, we had to abandon the ansatz used in Refs. [21, 34, 35, 23]. A more careful treatment then leads to a theory of multilead geometries with or without symmetries which reproduces and generalizes the results of Section 2. The Fano function arises as the most general resonance lineshape, under the assumption that the background can be considered constant over the width of the resonace. The Breit-Wigner lineshape appears as a special case when the nonresonant channels with which the resonant scattering can interfere suffer no phase shifts.

As a result of our comparison between scattering in two-dimensional rotationally invariant systems and symmetric Q1D structures in the single-subband regime, we saw that in both cases we could classify resonances according to the irreducible representations of the respective symmetry groups. For continuous symmetry, the asymmetry of the resonance lineshape depends only on the phase shift for direct (nonresonant) scattering in the angular momentum channel that exhibits the resonance. The phase shifts in all other angular momentum channels simply give rise to a baseline in the total cross section but do not interfere with the resonant scattering. The situation is different for discrete symmetries, in that the nonresonant phase shifts of *all* channels influence the lineshape asymmetry through interference. The reason for this is that we measure cross sections in two and three dimensions, but conductance coefficients (or transmission probabilities)

28

in Q1D systems. These quantities do not become equivalent in the limit of infinitely many leads. In fact, the effect of a resonance in Q1D vanishes with increasing number N of leads. More precisely, both the total transmission and individual S-matrix elements vary by at most $4(N-1)/N^2$ which is less than unity for $N > 2$.

More generally, we find that independent of the number of subbands *or* leads, the total transmission of a Q1D structure cannot vary by more than unity when a resonance is crossed. But the well-known result for resonances in resonant-tunneling structures [21, 22, 23], that the total transmission of a two-probe structure varies *exactly* by one if the system is symmetric, does not remain valid in general. As an example for this consider a ballistic constriction. If there is only one propagating subband, Gurvitz and Levinson [19] predict the occurrence of exact transmission zeros (antiresonances) on the conductance plateau close to the second subband threshold. This does *not* generalize to higher plateaus, i.e. an antiresonance on a higher quantized plateau cannot dip all the way down to the level of the previous plateau. We were able to derive this because our approach allows us to consider two-probe structures with more than one propagating subband as well. Our predictions are consistent with numerical calculations [41]. Moreover, we can now state that the lineshape will be of the *asymmetric* Fano lineshape if the plateau is not well quantized or if the resonance occurs in the step region.

The elastic Fano resonance obeys a scaling property in that lineshapes with different width Γ fall onto a single curve when plotted in reduced units ϵ, provided the background transmission is the same. This effect can be tested in transport experiments if one has a means of varying Γ without significantly altering the background transmission. The two model systems we discuss (quantum well and quantum groove in a magnetic field) have this property, but direct observation of the Fano lineshape is possible only in the quantum well configuration.

A. SOLUTION OF THE COUPLED CHANNEL EQUATIONS

In this Appendix we solve the coupled channel equations Eqs. (10,11) with the ansatz of Eq. (12), namely $\psi_2(x) = A\,\Phi_0(x)$. Inserting this into Eq. (10), we get an inhomogenous equation for $|\psi_1\rangle$ which can be solved with the retarded Green's operator (no label is necessary to distinguish it from its advanced counterpart since the latter is not used here)

$$\hat{G}_1 \equiv \left[E - E_1 - \hat{K} - U - \hat{V}_{11} + i\,0^+\right]^{-1}. \tag{87}$$

Acting with this on Eq. (10), the general solution to that inhomogenous equation is found to be

$$|\psi_1\rangle = |\chi_k^1\rangle + A\,\hat{G}_1\,\hat{V}_{12}\,|\Phi_0\rangle. \tag{88}$$

With this, Eq. (11) becomes

$$A(E - E_0)|\Phi_0\rangle = \hat{V}_{21} |\chi_k^1\rangle + A \hat{V}_{21} \hat{G}_1 \hat{V}_{12} |\Phi_0\rangle, \tag{89}$$

which can be closed with $\langle\Phi_0|$ to get

$$A = \frac{\langle\Phi_0|\hat{V}_{21} |\chi_k^1\rangle}{E - E_0 - \langle\Phi_0|\hat{V}_{21} \hat{G}_1 \hat{V}_{12} |\Phi_0\rangle} \tag{90}$$

and finally

$$|\psi_1\rangle = |\chi_k^1\rangle + \hat{G}_1 \hat{V}_{12} |\Phi_0\rangle \frac{\langle\Phi_0|\hat{V}_{21} |\chi_k^1\rangle}{E - E_0 - \langle\Phi_0|\hat{V}_{21} \hat{G}_1 \hat{V}_{12} |\Phi_0\rangle}. \tag{91}$$

Using the explicit form of the retarded Green's function in one dimension, [42]

$$G_1(x, x') = \frac{m}{i\hbar^2 k t^{bg}} \begin{cases} \chi_k^1(x) \chi_k^2(x') & (x > x') \\ \chi_k^1(x') \chi_k^2(x) & (x < x'), \end{cases} \tag{92}$$

we obtain for $x \to \infty$

$$\psi_1(x) = \chi_k^1(x) + \frac{m}{i\hbar^2 k t^{bg}} \chi_k^1(x) \frac{\langle(\chi_k^2)^*|\hat{V}_{12} |\Phi_0\rangle\langle\Phi_0|\hat{V}_{21} |\chi_k^1\rangle}{E - E_0 - \langle\Phi_0|\hat{V}_{21} \hat{G}_1 \hat{V}_{12} |\Phi_0\rangle} \tag{93}$$

and for $x \to -\infty$

$$\psi_1(x) = \chi_k^1(x) + \frac{m}{i\hbar^2 k t^{bg}} \chi_k^2(x) \frac{\langle(\chi_k^1)^*|\hat{V}_{12} |\Phi_0\rangle \langle\Phi_0|\hat{V}_{21} |\chi_k^1\rangle}{E - E_0 - \langle\Phi_0|\hat{V}_{21} \hat{G}_1 \hat{V}_{12} |\Phi_0\rangle}. \tag{94}$$

The matrix element in the denominator of Eq. (93) is a self energy due to the coupling between bound state and continuum, and will be denoted by

$$\langle\Phi_0|\hat{V}_{21} \hat{G}_1 \hat{V}_{12} |\Phi_0\rangle \equiv \Delta - i\Gamma, \tag{95}$$

where Δ and Γ are real. It is of crucial importance for the existence of exact transmission zeros that the numerator,

$$\frac{m}{i\hbar^2 k t^{bg}} \langle(\chi_k^2)^*|\hat{V}_{12} |\Phi_0\rangle \langle\Phi_0|\hat{V}_{21} |\chi_k^1\rangle \equiv \delta - i\Gamma, \tag{96}$$

has the same imaginary part $-\Gamma$, but in general a different real part, δ. The proof cannot proceed as in Ref. [19] when we admit a more general $\hat{V}^{xy}$, as is needed for magnetic-field induced coupling. Here we provide a generalized proof that requires the hermiticity of $\hat{V}^{xy}$ and the additional property $\hat{V}_{nl}^* = \pm\hat{V}_{nl}$. This is sufficient for the application we investigate in Subsection 2.3.

Using the definition of the Green's function, Eq. (92), we can rewrite the lefthand side in Eq. (95) as

$$\frac{m}{i\hbar^2 k t^{bg}} \int dx\, dx'\, \chi_k^2(x')\hat{V}_{12}^{x'}\, \Phi_0(x')\, \Phi_0(x)\, \hat{V}_{21}^x\, \chi_k^1(x) \tag{97}$$

$$= \frac{m}{i\hbar^2 k t^{bg}} \left(\int\limits_{x>x'} dx\, dx' + \int\limits_{x<x'} dx\, dx' \right) \Phi_0(x)\, \hat{V}_{21}^x\, \chi_k^1(x)\, \chi_k^2(x')\hat{V}_{12}^{x'}\, \Phi_0(x')$$

$$= \langle\Phi_0|\hat{V}_{21}\, \hat{G}_1\, \hat{V}_{12}\, |\Phi_0\rangle + \frac{m}{i\hbar^2 k t^{bg}} \int\limits_{x<x'} dx\, dx'\, \Phi_0(x)\, \hat{V}_{21}^x\, \chi_k^1(x)\, \chi_k^2(x')\hat{V}_{12}^{x'}\, \Phi_0(x')$$

$$- \frac{m}{i\hbar^2 k t^{bg}} \int\limits_{x<x'} dx\, dx'\, \Phi_0(x)\, \hat{V}_{21}^x\, \chi_k^2(x)\, \chi_k^1(x')\hat{V}_{12}^{x'}\, \Phi_0(x')$$

$$= \langle\Phi_0|\hat{V}_{21}\, \hat{G}_1\, \hat{V}_{12}\, |\Phi_0\rangle$$
$$+ \frac{m}{i\hbar^2 k t^{bg}} \int\limits_{x<x'} dx\, dx'\, \Phi_0(x)\, \hat{V}_{21}^x\, \left[\chi_k^1(x)\, \chi_k^2(x') - \chi_k^2(x)\, \chi_k^1(x')\right]\, \hat{V}_{12}^{x'}\, \Phi_0(x').$$

The difference in brackets can be written with the help of Eqs. (A14) of Ref. [19] as

$$\frac{1}{(t^{bg})^*} \left[\chi_k^1(x)\, \chi_k^1(x')^* - \chi_k^1(x)^*\, \chi_k^1(x')\right] = \frac{i}{(t^{bg})^*}\, f(x,x'), \tag{98}$$

where $f(x,x') \equiv 2\,\mathrm{Im}\left[\chi_k^1(x)^*\, \chi_k^1(x')\right]$ is real and satisfies $f(x,x') = -f(x',x)$. We therefore have to show that

$$\int\limits_{x<x'} dx\, dx'\, \Phi_0(x)\, \hat{V}_{21}^x\, f(x,x')\, \hat{V}_{12}^{x'}\, \Phi_0(x') \tag{99}$$

is real. This is immediately clear if $\hat{V}_{12}^{x'}$ and $\hat{V}_{21}^x$ are either both real or both imaginary. The latter happens if they are proportional to $p_x = -i\hbar\partial/\partial x$, e.g., and this is the case in the example studied in Section 2.3. Therefore, we conclude for the matrix elements occuring in Eq. (93) that

$$\frac{m}{i\hbar^2 k t^{bg}} \langle(\chi_k^2)^*|\hat{V}_{12}\, |\Phi_0\rangle\, \langle\Phi_0|\hat{V}_{21}\, |\chi_k^1\rangle = \langle\Phi_0|\hat{V}_{21}\, \hat{G}_1\, \hat{V}_{12}\, |\Phi_0\rangle + \delta, \tag{100}$$

where δ is real.

Using Eq. (8) for the scattering states, we get for $x \to \infty$

$$\psi_1(x) = t^{bg}\, e^{ikx} \left[1 + \frac{\delta - i\Gamma}{E - E_0 - \Delta + i\Gamma}\right] \tag{101}$$

which leads to the new transmission coefficient

$$T = |t^{bg}|^2 \left|1 + \frac{\delta - i\Gamma}{E - E_0 - \Delta + i\Gamma}\right|^2 \tag{102}$$

$$= |t^{bg}|^2 \frac{(E - E_0 - \Delta + \delta)^2}{(E - E_0 - \Delta)^2 + \Gamma^2}. \tag{103}$$

B. REFLECTION ZEROS IN SYMMETRIC STRUCTURES

The scattering state given by Eq. (91) is normalized to the same incident flux as $|\chi_k^1\rangle$ because $G_1(x, x')$ only adds outgoing waves originating from point sources at x' in the region of the bound state. Thus, current conservation must hold for the reflection and transmission probabilities in the presence of coupling, $R + T = 1$. Let us now consider the reflection R. Using Eq. (A 14) of Ref. [19] and the asymptotic form of χ_k^2 we can rewrite Eq. (94) as

$$
\begin{aligned}
\psi_1(x) &= e^{ikx} + r_+^{bg} e^{-ikx} + \\
&\quad \frac{m}{i\hbar^2 k} e^{-ikx} \frac{\left[r_+^{bg}/t^{bg}\langle(\chi_k^2)^*|\hat{V}_{12}|\Phi_0\rangle + 1/(t^{bg})^*\langle\chi_k^2|\hat{V}_{12}|\Phi_0\rangle\right]\langle\Phi_0|\hat{V}_{21}|\chi_k^1\rangle}{E - E_0 - \langle\Phi_0|\hat{V}_{21}\hat{G}_1\hat{V}_{12}|\Phi_0\rangle} \\
&= e^{ikx} + \\
&\quad r_+^{bg} e^{-ikx} \left[1 + \frac{\delta - i\Gamma + m/(i\hbar^2 k r_+^{bg}(t^{bg})^*)\langle\chi_k^2|\hat{V}_{12}|\Phi_0\rangle\langle\Phi_0|\hat{V}_{21}|\chi_k^1\rangle}{E - E_0 - \Delta + i\Gamma}\right],
\end{aligned}
\tag{104}
$$

where the definition Eq. (95) was used.

In an inversion symmetric structure, the remarks in Section 2.2 together with the hermiticity of $\hat{V}^{xy}$ lead to the conclusion that the remaining combination of matrix elements in Eq. (104),

$$
\eta \equiv \frac{m}{i\hbar^2 k r(t^{bg})^*}\langle\chi_k^2|\hat{V}_{12}|\Phi_0\rangle\langle\Phi_0|\hat{V}_{21}|\chi_k^1\rangle
\tag{105}
$$

is real because

$$
\langle\chi_k^2|\hat{V}_{12}|\Phi_0\rangle = \pm\langle\Phi_0|\hat{V}_{21}|\chi_k^1\rangle^*.
\tag{106}
$$

The reflection probability thus has the form

$$
R = |r^{bg}|^2 \left|1 + \frac{\delta - i\Gamma + \eta}{E - E_0 - \Delta + i\Gamma}\right|^2
\tag{107}
$$

$$
= |r^{bg}|^2 \frac{(E - E_R + \delta + \eta)^2}{(E - E_R)^2 + \Gamma^2},
\tag{108}
$$

where we have again used the shifted resonance energy $E_R = E_0 + \Delta$. This shows that R indeed goes to zero in the presence of inversion symmetry, implying $T = 1$. The distance between the points of unit and zero transmission is η, as can be seen from comparison with Eq. (103). Imposing the condition $R + T = 1$ yields

$$
\delta = -|r^{bg}|^2\eta, \qquad \Gamma^2 = |r^{bg}\,t^{bg}|^2\eta^2.
\tag{109}
$$

From this we obtain Eq. (17). Instead of q, we could also use t^{bg} as the third lineshape parameter. For a given resonance, E_R and η can be read off directly from the positions of the minimum and maximum, while $|t^{bg}|^2$ is the transmission baseline away from resonance. If $|t^{bg}|^2$ is not exactly constant, one has to find the best fit by interpolating between the values of $|t^{bg}|^2$ to the left and right of the resonance.

C. TUNING THE FERMI ENERGY WITH A MAGNETIC FIELD

Here we discuss the dependence of the Fermi energy on the magnetic field, neglecting disorder. Consider a three-dimensional electron gas (effective mass m^*) in a homogenous magnetic field along the z axis: the energy eigenvalues are

$$E_n = \hbar\omega_c \left(n - \frac{1}{2}\right) + \frac{\hbar^2 k_z^2}{2m^*} \pm \frac{1}{2} g^* \mu_B B \quad (n = 1, 2, \ldots) \tag{110}$$

and have a degeneracy per unit area (perpendicular to the magnetic field) of

$$D = \frac{eB}{hc} \tag{111}$$

We want to determine the Fermi energy at $T = 0$ for a given electron density ρ which is fixed by the doping. First consider fully spin-polarized electrons in the lowest LL. Only the low-energy Zeeman term in Eq. (110) is then relevant, so that the minimum energy is

$$E_0 \equiv \frac{1}{2}\hbar\omega_c - \frac{1}{2}|g^*\mu_B B| = \frac{1}{2}\hbar\omega_c \left(1 - \alpha\right), \tag{112}$$

where we defined $\eta \equiv |g^*| \, m^*/2m_e$ which determines the Zeeman splitting, and assumed $B > 0$. If $\alpha < 1$, the spin splitting is less than the cyclotron frequency $\omega_c \equiv eB/m^*c$. The density must satisfy

$$\rho = D \int_{E_0}^{E_F} g(E)\, dE \tag{113}$$

with the one-dimensional density of states,

$$g(E) = \frac{1}{2\pi} \left[\frac{\hbar^2}{2m^*} \left(E - E_0\right)\right]^{-\frac{1}{2}}. \tag{114}$$

The integral yields

$$\rho = \frac{eB}{\pi hc} \left[\frac{2m^*}{\hbar^2} \left(E_F - E_0\right)\right]^{\frac{1}{2}}, \tag{115}$$

so that the Fermi energy as a function of magnetic field becomes

$$E_F = \frac{1}{2}\hbar\omega \left(1 - \eta\right) + \frac{\hbar^2}{2m^*} \left(\frac{\pi\rho hc}{eB}\right)^2. \tag{116}$$

This relation is correct only if E_F is in the spin-polarized lowest LL, so that the magnetic field has to be greater than a threshold field determined by the condition

$$E_F = \frac{1}{2}\hbar\omega + \min(\frac{1}{2}|g^*\mu_B B|\,\hbar\omega - \frac{1}{2}|g^*\mu_B B|) = \frac{1}{2}\hbar\omega_c \left(1 + \min(\eta, 2 - \eta)\right). \tag{117}$$

Equating this with Eq. (116), one obtains an expression for the threshold field,

$$B_0 = \left(\frac{\pi \rho^2}{4 \min(1, \eta)} \right)^{\frac{1}{3}} \frac{hc}{e}.$$ (118)

In view of the specific example treated in this paper, we assume $\eta < 1$ from now on. This does not affect the basic mechanism. In units of B_0, we can rewrite Eq. (116) as

$$E_F = \hbar \omega_c \left[\frac{1}{2} (1 - \eta) + \eta \left(\frac{B_0}{B} \right)^3 \right] \qquad (B \geq B_0).$$ (119)

For InSb with its strong spin-orbit coupling [43], one has $\eta \approx 1/3$ so that we estimate $B_0 \approx 12T$ if the doping is $\rho = 10^{-7} \text{ cm}^{-3}$. The Zeeman splitting is then $\hbar \eta \omega_c = \hbar \omega_c / 3$.

Now we consider how E_F behaves when $B < B_0$, so that both spin directions are present. We still assume that only the lowest LL is populated. In straightforward generalization of the previous procedure, E_F must now satisfy

$$\rho = \frac{1}{\pi} \frac{eB}{hc} \sqrt{\frac{2m}{\hbar^2}} \left[\sqrt{E_F - \frac{1}{2}\hbar \omega_c + \frac{1}{2} g^* \mu_B B} + \sqrt{E_F - \frac{1}{2}\hbar \omega_c - \frac{1}{2} g^* \mu_B B} \right].$$ (120)

Here, the two terms in square brackets count the number of spin-up and spin-down electrons below E_F, respectively. Solving this for E_F,

$$E_F = \hbar \omega_c \left[\frac{1}{2} + \frac{1}{2} \frac{\pi^4 \hbar^3 \rho^2}{m^3 \omega_c^3} + \frac{1}{8} \eta^2 \frac{m^3 \omega_c^3}{\pi^4 \hbar^3 \rho^2} \right],$$ (121)

The assumption that E_F is below the second LL threshold will be valid for magnetic fields greater than the minimum value determined by

$$E_F = \frac{3}{2}\hbar \omega_c - \frac{1}{2} g^* \mu_B B = \frac{1}{2}\hbar \omega_c (3 - \eta).$$ (122)

The solution for this threshold field is

$$B_{th}^3 = \frac{\pi}{2} \rho^2 \left(\frac{hc}{e} \right)^3 \left(\frac{1}{\eta} \right)^2 \left(1 - \frac{1}{2}\eta - \sqrt{1 - \eta} \right).$$ (123)

At $\rho = 10^{17} \text{cm}^{-3}$ in InSb one obtains for the threshold field the value $B_{th} \approx 5.0T$. Using the threshold field for spin polarization, B_0, as a unit, one can write the Fermi energy as

$$E_F = \frac{1}{2}\hbar \omega_c + \frac{1}{4}\hbar \omega_c \eta \left[\left(\frac{B_0}{B} \right)^3 + \left(\frac{B}{B_0} \right)^3 \right] \qquad (B_{th} \leq B \leq B_0).$$ (124)

The function given by Eq. (119) and Eq. (124) is plotted in the inset to Fig. 5.

References

[1] R. Landauer, Z. Phys. **68**, 217 (1987); M. Büttiker, IBM J. Res. Develop. **32**, 317 (1988)

[2] M. Büttiker, Phys. Rev. A **30**, 1982 (1984)

[3] D. Y. K. Ko and J. C. Inkson, Semicond. Sci. Technol. **3**, 791 (1988)

[4] R. L. Schult, H. D. Wyld and D. G. Ravenhall, Phys. Rev. B **41**, 12760 (1990)

[5] P. F. Bagwell, Phys. Rev. B **41**, 10354 (1990)

[6] H. U. Baranger, Phys. Rev. B **42**, 11479 (1990)

[7] W. Porod, Zhi-an Shao and C. S. Lent, Appl. Phys. Lett. **61**, 1350 (1992)

[8] P. F. Bagwell and R. K. Lake, Phys. Rev. B **46**, 15329 (1992)

[9] J. U. Nöckel, Phys. Rev. B **46**, 15348 (1992)

[10] D. Z. Y. Ting and T. C. McGill, Phys. Rev. B **47**, 7281 (1993)

[11] E. Tekman and P. Bagwell, Phys. Rev. B **48**, 2553 (1993)

[12] G. Breit and E. Wigner, Phys. Rev. **49**, 519 (1936)

[13] U. Fano, Phys. Rev. **124**, 1866 (1961)

[14] J. A. Simpson and U. Fano, Phys. Rev. Lett. **11**, 158 (1963)

[15] R. K. Adair, C. K. Bockelman and R. E. Peterson, Phys. Rev. **76**, 308 (1949)

[16] J. M. Blatt and V. F. Weisskopf, *Theoretical Nuclear Physics* (Wiley, New York, 1952), chapter VIII.

[17] H. Friedrich, *Theoretical Atomic Physics* (Springer Verlag, Berlin 1990)

[18] J. U. Nöckel and A. D. Stone, unpublished

[19] S. A. Gurvitz and Y. B. Levinson, Phys. Rev. B **47**, 10578 (1993)

[20] H. Feshbach, Ann. Phys. **5** 357 (1958); Ann. Phys. **19** 287 (1962)

[21] M. Büttiker, IBM J. Res. Develop. **32**, 63 (1988); Phys. Rev. B **38**, 12724 (1988)

[22] M. Sumetskii, J. Phys.: Condens. Matter **3**, 2651 (1991)

[23] P. J. Price, Phys. Rev. B **48**, 17301 (1993)

[24] Z. Shao, W. Porod, C. S. Lent, Phys. Rev. B **49**, 7453 (1994)

[25] P. L McEuen, B. W. Alphenaar, R. G. Wheeler and R. N. Sacks, Surf. Sci **229**, 312 (1990).

[26] C. H. Lewenkopf and H. A. Weidenmüller, Ann. Phys. **212** 53 (1991)

[27] Since $|t^{bg}|^2$ is the transmission of a hypothetical system without coupling to the bound state, the transmission T of the real system will approach $|t^{bg}|^2$ whenever this coupling is negligible, i.e. at energies far away from the bound level. Over the width of the resonance, T varies strongly while $|t^{bg}|^2$ is often approximately constant. The latter assumption is not crucial in our calculations, but the exact Fano lineshape results only if t^{bg} is constant on resonance.

[28] The bound state energy need not be close to E_2 as stated in Ref. [19].

[29] The result that the energy shifts depend on ω_c only through even powers can also be derived purely from symmetry considerations because Eq. (21) is invariant under simultaneous reversal of magnetic field and $y \rightarrow -y$, so that the transmission at given E cannot depend on the sign of ω_c.

[30] The stub structure with purely one-dimensional waveguides has been treated within a two-channel framework in Ref. [11], but the authors remark that the approximation they make does not lead to a very realistic physical mechanism.

[31] P. J. Price, Phys. Rev. B **38**, 1994 (1988)

[32] In Ref. [8] it is erroneously stated that the metastable state must exhibit exponential decay in the leads. This may be the reason why Ref. [11] chooses the branch cuts for the wavenumber in the complex energy plane in a very unconventional way that even depends on the position of the poles of S. There is, in fact, nothing that prevents us from choosing the cut along the negative real axis. A metastable state with exponential decay in the leads would violate conservation of matter because its probability integral decreases with time. Exponential growth in the leads is admissible, cf. Ref. [16], because the resulting normalization integral is always infinite.

[33] T. Berggren, Nucl. Phys. **109 A**, 265 (1968)

[34] J. R. Taylor, *Scattering Theory* (Wiley, New York, 1972)

[35] L. D. Landau and E. M. Lifshitz, *Quantum Mechanics, Non-relativistic Theory* (Pergamon Press, Oxford, 1977), chapter XVIII.

[36] This happens when the last sum in Eq. (71) contains only terms that describe symmetric lineshapes, but some of them are dips and some are peaks. Adding these with different prefactors Q_j^2 results in a symmetric lineshape with a variation $\Delta T < 1$.

[37] V. Kalmeyer and R. B. Laughlin, Phys. Rev. B **35**, 9805 (1987)

[38] G. Timp, in: *Physics of Nanostructures*, J. H. Davies and A. R. Long (eds.), SUSSP proceedings, Institute of Physics Publishing, Bristol and Philadelphia (1992)

[39] J. U. Nöckel, Phys. Rev. B **45**, 14225 (1992)

[40] H. L. Stormer *et al.*, in *Nanostructures and Mesoscopic Systems* (Academic Press 1992)

[41] J. A. Nixon, J. H.Davies, H. U. Baranger, Phys. Rev. B **43**, 12638 (1991)

[42] R. Courant and D. Hilbert, *Methoden der mathematischen Physik*, Vol. I, (Springer Verlag, Berlin 1968)

[43] K. H. Hellwege (ed.), *Landolt-Börnstein. Numerical Data and Functional Relationships in Science and Technology*, Vol. 17a (Springer Verlag, Berlin, 1982)